

# Analytic and Finite Element Solutions for Temperature Profiles in Welding using Varied Heat Source Models

Djarot B. Darmadi, John Norrish and Anh Kiet Tieu

**Abstract**—Solutions for the temperature profile around a moving heat source are obtained using both analytic and finite element (FEM) methods. Analytic and FEM solutions are applied to study the temperature profile in welding. A moving heat source is represented using both point heat source and uniform distributed disc heat source models. Analytic solutions are obtained by solving the partial differential equation for energy conservation in a solid, and FEM results are provided by simulating welding using the ANSYS software. Comparison is made for quasi steady state conditions. The results provided by the analytic solutions are in good agreement with results obtained by FEM.

**Keywords**—Analytic solution, FEM, Temperature profile, Heat Source Model

## I. INTRODUCTION

WELDING applications subject welded materials to non-uniform temperature cycle. This non-uniformity causes problems which in turn lead to premature fatigue damage, stress corrosion and fracture [1]. Studies on temperature distributions as well as temperature histories become very important in the actual process control in welding which still faces many problems.

Weld modeling using analytic solutions or numerical approaches is commonly employed today. Those models are used to exhibit what is called ‘intellectual control’ [2], as an alternative to in-process control which may be difficult to apply in some welding processes. After Rosenthal demonstrated an analytic solution for a moving point heat source, analytical models were widely applied [3]-[8]. With the advent of more powerful computers, numerical methods such as FEM have been more frequently used. An advantage of numerical analysis over analytic method is the possibility to obtain solution for complex condition (e.g. geometry, border conditions) which may be difficult by analytic solution. However, analytic solutions have continued to be developed since they allow a better understanding of the underlying processes and fast solutions once the analytic solution is established. Analytic solution can also be used to verify FEM results. The current paper attempts to combine the two

approaches and the results for quasi steady state is compared.

Analytic solutions to welding heat flow problems are obtained by solving the partial differential equation of energy conservation (1).  $T$  is the temperature;  $x, y$  and  $z$  are the three mutually orthogonal directions;  $\alpha$  is the diffusivity;  $t$  is the time. Steady state solutions can be obtained by allowing time  $t \rightarrow \infty$ .

$$\frac{\partial^2 T}{\partial x^2} + \frac{\partial^2 T}{\partial y^2} + \frac{\partial^2 T}{\partial z^2} = \frac{1}{\alpha} \frac{dT}{dt} \quad (1)$$

Rosenthal [3] developed quasi steady state solutions for a moving heat source by observing temperature distribution around coordinates which coincided with the moving heat source. Theoretically, after a certain time has elapsed, the temperature at given position relative to the moving coordinate is steady and therefore the condition is called ‘quasi steady state’.

Komanduri and Hou [8] developed non-dimensional integral to carry out thermal analysis in welding. He used Gaussian distributed moving disc heat source to represent heat load which embeds by weld torch. Solution for the non-dimensional integration is obtained through numerical approach.

FEM analysis was carried out by simulating the welding model using ANSYS 12.0. The quasi steady state is observed by evaluating temperature distribution around moving coordinates, coinciding with the welding torch, when moving heat source models have travelled a long enough distance from start point.

The moving heat source is modeled as moving point heat source and uniformly distributed disc heat source. The point heat source considers a moving point with heat rate value equal to  $\dot{q}$ . The uniformly distributed disc heat source with outside radius  $r_o$ , considers the heat source has uniform heat flux rate value  $\dot{q}'' = \dot{q} / (\pi r_o^2)$  over a circle on a plate surface.

Analytic solutions, in this paper, are developed based on proposed solution by Carslaw and Jaeger [4]. Following the method that was used by Komanduri and Hou [8], non dimensional definite integral is used to obtain solutions for point heat source and uniformly distributed disc heat source whilst Komanduri and Hou obtained solution based on Gaussian distributed disc heat source model. Solutions obtained from the analytic solution are combined with

Darmadi, Djarot is a senior Brawijaya University (Indonesia) lecturer. E-mail: b\_darmadi\_djarot@yahoo.co.id.

Norrish, J. is a professor of welding at University of Wollongong, Australia.

Kiet Tieu, A. is a professor of mechanical engineering at University of Wollongong, Australia.

solutions obtained from FEM simulation and the results for quasi-steady state are compared.

## II. ANALYTIC SOLUTIONS

### A. Solutions by Rosenthal

Rosenthal has proposed solution for moving point heat source which is expressed in (2), where  $v$  is the welding speed. The proposed solution is based on the shape of weld-pool. Since (2) is not a time ( $t$ ) function, it is a solution for quasi steady state. Quasi steady state is steady state if parameters are considered from moving coordinates  $(\xi, y', z')$ . The fix coordinate system is expressed as  $(x, y, z)$  which is following right hand rule. The coordinates are described in Fig. 1. Since the heat source is moving parallel to  $x$  axis, the value of  $y'$  equal to  $y$  and the value of  $z'$  equal to  $z$ . For convenience, instead of expressing a position of a point as  $(\xi, y', z')$  in the moving abscissa system, it is expressed as  $(\xi, y, z)$ .

$$\Delta T = \exp(-v\xi/(2\alpha))f(\xi, y', z') \quad (2)$$

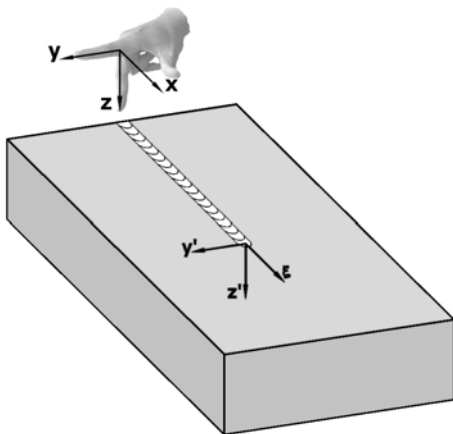


Fig. 1 Fixed coordinate system and moving coordinate system

Equation (2) comprise of asymmetric function, it is  $\exp(-v\xi/(2\alpha))$  and symmetric function:  $f(\xi, y', z')$ . Asymmetric function is found along lines parallel to  $\xi$  and symmetric function is found along both: lines which parallel to  $y$  and parallel to  $z$ . If welding speed equals to zero the asymmetric function will be a unity and only symmetric function is left. Zero welding speed means a case of heat liberated by a stationary point which has solution much easier than moving point heat source. A final solution proposed by Rosenthal for moving point heat source for semi infinite solid is expressed in (3).  $k$  is the conductivity and  $R$  is the distance from heat source.  $T_0$  is added to consider initial temperature of welded plate. Symmetric function of (3) is  $\dot{q}/(2\pi kR) \cdot \exp(-vR/(2\alpha))$ .

$$T = T_0 + \dot{q}/(2\pi kR) \exp(-v(R + \xi)/(2\alpha)) \quad (3)$$

It should be noted that the temperature at weld center, which is obtained by replacing  $R$  and  $\xi$  with zero, is infinite. It does not make sense in a real condition but found in theoretical approach.

### B. Non dimensional integral by Komanduri and Hou

Carslaw and Jaeger have proposed a solution for instantaneous point heat source that liberates heat at  $(x_0, y_0, z_0)$  as it is expressed in (4).  $\phi$  is a function which depends on heat load and material thermal properties.

$$T = \phi / (8(\pi\alpha t)^{3/2}) \cdot \exp\left[-\frac{\{(x-x_0)^2 + (y-y_0)^2 + (z-z_0)^2\}}{4\alpha t}\right] \quad (4)$$

Based on the proposed solution in (4), Komanduri and Hou [8] obtained solutions for temperature distribution around Gaussian distributed disc heat source as it is expressed in (5).

$$T - T_0 = 3.1576 \dot{q} v / (4k\alpha\pi^{3/2}r_0^2) \cdot \exp(-\xi V) \cdot \int_{r_i=0}^{r_0} \exp(-3(r/r_0)^2) r dr \cdot \int_{\omega=0}^{v^2 t / 4\alpha} I_0\left(\frac{r_i V^2}{2\omega} \sqrt{(\xi + 2\omega/V)^2 + y^2}\right) \exp(-(\omega + u^2/(4\omega)) \frac{d\omega}{\omega^{3/2}}) \quad (5)$$

where  $\omega = v^2 \tau / (4\alpha)$ ,  $R_h^2 = \xi^2 + y^2 + z^2 + r^2$ ,  $V = v / (2\alpha)$ ,  $u = R_h V$ ,  $v\tau = 2\omega / V$  and  $I_0(p)$  is modified Bessel function first kind, order zero. Since  $\omega$  is a non-dimensional term, equation (5) is called as non-dimensional integral.

### C. Proposed solution for moving point heat source

Following the method that was used by Komanduri and Hou, solutions for moving point heat source is based on (4). If heat source is liberated at origin, equation (4) will be simpler as it is expressed in (6).

$$T = \phi / (8(\pi\alpha t)^{3/2}) \cdot \exp\left\{-\frac{(x^2 + y^2 + z^2)}{4\alpha t}\right\} \quad (6)$$

The total heat for an infinite solid liberated by the heat source can be expressed as in (7), where  $\rho$  is the density and  $c$  is the specific heat.

$$\dot{q} dt = \int_{-\infty}^{\infty} \rho c T dx dy dz \quad (7)$$

Substituting  $T$  which is expressed in (6) to (7) yields  $\phi = \dot{q} dt / (\rho c)$ . As a result (6) can be written as in (8).

$$T = \dot{q} dt / (8\rho c (\pi\alpha t)^{3/2}) \cdot \exp\left\{-\frac{(x^2 + y^2 + z^2)}{4\alpha t}\right\} \quad (8)$$

The temperature rise resulting from a moving point heat source which was initially at origin (0,0,0) and moving parallel to the x axis at a constant speed (Fig. 2), can be obtained based on equation (8). Equation (8) can be interpreted as temperature rise in infinite solid due to instantaneous heat liberated when  $t = 0$  at origin. When  $t \rightarrow 0$  temperatures at all points are zero except at origin which is infinite.

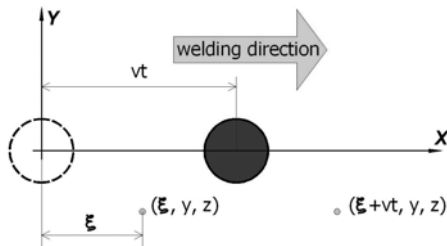


Fig. 2 Point heat source in infinite media

Equation (9) is obtained by adjust (8) to a moving coordinates which coincide with the moving heat source and temperature rise in a small time increment is expressed as  $dT$ .

$$dT = \dot{q} dt / (8\rho c (\pi\alpha t)^{3/2}) \exp\left\{-\left(\left(\xi + vt\right)^2 + y^2 + z^2\right) / (4\alpha t)\right\} \quad (9)$$

The total temperatures rise at any points can be obtained by integrating (8) and considering initial temperature as  $T_0$ . The temperature rise is expressed in (10).

$$T - T_0 = \dot{q} / (8\rho c (\pi\alpha)^{3/2}) \int_{\tau=0}^t \frac{\exp\left\{-\left(\left(\xi + v\tau\right)^2 + y^2 + z^2\right) / 4\alpha\tau\right\}}{\tau^{3/2}} d\tau \quad (10)$$

This integration can be expressed in the non-dimensional form by substituting the following expressions:  $\omega = v^2 \tau / (4\alpha)$ ,  $R_h^2 = \xi^2 + y^2 + z^2$ ,  $V = v / (2\alpha)$ ,  $u = R_h V$ ,  $v\tau = 2\omega / V$  and equation (11) is obtained.

$$T - T_0 = \dot{q} v \exp(-\xi V) / (16\rho c \alpha^2 \pi^{3/2}) \int_{\omega=0}^{v^2 t / 4\alpha} \frac{e^{-\left(\omega - \frac{u^2}{4\omega}\right)}}{\omega^{3/2}} d\omega \quad (11)$$

For a semi-infinite solid case as in welding, the temperature which is obtained by (11) should be doubled because the heated volume is a half of an infinite solid. For convenience  $\rho c$  is replaced by  $k/\alpha$ . Temperatures for any points in welding model can be represented by (12).

$$T = T_0 + \dot{q} v \exp(-\xi V) / (8k\alpha\pi^{3/2}) \int_{\omega=0}^{v^2 t / 4\alpha} \frac{\exp\left(-\omega - \frac{u^2}{4\omega}\right)}{\omega^{3/2}} d\omega \quad (12)$$

The values for the definite integral in equation (12) depend on the upper limit value which is a time function. Clearly, equation (12) is the solution for a transient state and results for a quasi steady state can be found by replacing the value of  $t \rightarrow \infty$ , thus the upper integration limit is equal to  $\infty$ . Since when  $\omega = 0$  a singularity is found, the solution cannot be solved analytically but numerically by setting the lower limit close to 0 (e.g. 0.001). The integral expression in (11) is plotted and presented graphically in Fig. 3. From Fig.3 it can be concluded that when  $u \geq 3$  the values of the integral are numerically closed to zero which means that there is no significant temperature elevation. It can also be drawn from Fig. 3 that at a higher  $u$  value, the definite integration value is converged at a higher value of  $\omega$  (which also means a longer time). For lower  $u$  values, it was found that when  $\omega \geq 5$  the integral will be converged, thus it is enough if the upper limit of integration is considered as 5 which make the numerical solution much easier.

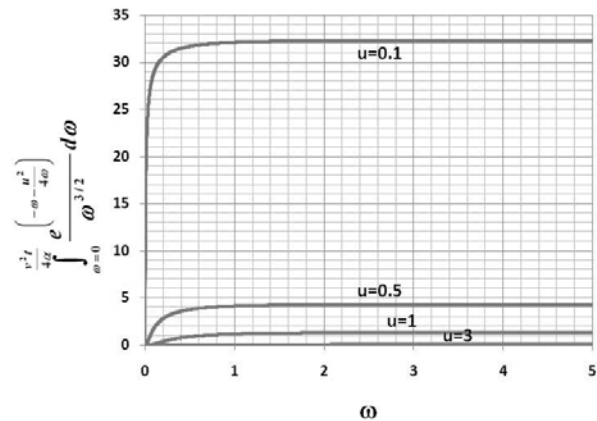


Fig. 3 Integral values for varied  $\omega$  and  $u$

#### D. Proposed solutions for uniformly distributed moving disc heat source

In surface heat source model, a uniformly distributed moving disc heat source is the simplest configuration. The temperature profile in an infinite solid with a moving uniformly distributed disc heat source can be obtained by developing a solution for an instantaneous ring heat source, with radius equal to  $r$ , as proposed by Carslaw and Jaeger which is represented in (13).

$$\Delta T = \dot{q}_r / (8\rho c (\pi\alpha t)^{3/2}) \exp\left\{-\left(r^2 + x^2 + y^2 + z^2\right) / (4\alpha t)\right\} I_0\left(r / (2\alpha t) \sqrt{x^2 + y^2}\right) \quad (13)$$

Converting to moving coordinates, for small time increment the temperature rise in (13) can be expressed as (14).

$$dT = \dot{q}_r / (8\rho c (\pi\alpha t)^{3/2}) dt \cdot \exp\left\{-\left(r^2 + (\xi + vt)^2 + y^2 + z^2\right)/(4\alpha t)\right\} \cdot I_0\left(r/(2\alpha t)\sqrt{(\xi + vt)^2 + y^2}\right) \quad (14)$$

The temperature profile resulting from a moving ring heat source can be obtained from (15) by integrating (14).

$$T - T_0 = \dot{q}_r / (8\rho c (\pi\alpha)^{3/2}) \int_{\tau=0}^t I_0\left(r/(2\alpha\tau)\sqrt{(\xi + v\tau)^2 + y^2}\right) \exp\left(-\left(r^2 + (\xi + v\tau)^2 + y^2 + z^2\right)/(4\alpha\tau)\right) \frac{d\tau}{\tau^{3/2}} \quad (15)$$

Substituting following expression:  $\omega = v^2\tau/(4\alpha)$ ,  $R_h^2 = r^2 + \xi^2 + y^2 + z^2$ ,  $V = v/2\alpha$ ,  $u = R_h V$ ,  $v\tau = 2\omega/V$  and replace  $\rho c$  with  $k/\rho$ ; the non-dimensional integral as in (16) can be obtained.

$$T - T_0 = \dot{q}_r v / (16k\alpha\pi^{3/2}) \cdot \exp(-\xi V) \cdot \int_{\omega=0}^{v^2 t / 4\alpha} I_0\left(rV^2/(2\omega)\sqrt{(\xi + 2\omega/V)^2 + y^2}\right) \exp\left\{-\left(\omega + u^2/(4\omega)\right)\right\} \frac{d\omega}{\omega^{3/2}} \quad (16)$$

Equation (15) is temperature rise in infinite solid due to ring heat source with radius equal to  $r$ . The temperature rise in semi-infinite solid should be twice than (16) as it is expressed in (17).

$$T - T_0 = \dot{q}_r v / (8k\alpha\pi^{3/2}) \cdot \exp(-\xi V) \cdot \int_{\omega=0}^{v^2 t / 4\alpha} I_0\left(rV^2/(2\omega)\sqrt{(\xi + 2\omega/V)^2 + y^2}\right) \exp\left\{-\left(\omega + u^2/(4\omega)\right)\right\} \frac{d\omega}{\omega^{3/2}} \quad (17)$$

The heat flux for a uniformly distributed disc with radius  $r_0$  is  $\dot{q}'' = \dot{q} / \pi r_0^2$ , and the heat rate liberated by incremental ring with radius  $r$  is  $\dot{q}(\pi r^2) \cdot 2\pi r dr$ . Using this expression, the temperature rise by a moving incremental ring over semi infinite solid can be expressed by (18).

$$T - T_0 = \dot{q} v r dr / (4r_0^2 k \alpha \pi^{3/2}) \cdot \exp(-\xi V) \int_{\omega=0}^{v^2 t / 4\alpha} I_0\left(r_0 V^2 / 2\omega \sqrt{(\xi + 2\omega/V)^2 + y^2}\right) \exp\left\{-\left(\omega + u^2/(4\omega)\right)\right\} \frac{d\omega}{\omega^{3/2}} \quad (18)$$

The total temperature rise for a uniformly distributed

circular heat source can be expressed by (19). Solving the first integration in (19) results in a temperature profile that can be expressed by (20). Equation (20) is the transient solution since values for the second integration depend on time  $t$ . The solution for the quasi steady state can be obtained by setting  $t$  or the upper limit of integration to  $\infty$ . Solving (20) analytically may be impossible since the singularity is existed when  $\omega = 0$ . By setting the lower limit close to zero (e.g. 0.001) the integration can again be solved numerically. As found with the point heat source, it is sufficient to set the upper limit of integral to 5 since integral values will be converged. This convergence is also demonstrated in a different way by Fig. 3 and is presented in Fig. 4 and Fig. 5. Fig. 4 and Fig. 5 present temperature profile which evaluates at a certain line. It can be seen from Fig. 4 which has used a line defined by  $y = 0$  mm and  $z = 10$  mm, when the upper time limit is  $t = 200$  s or  $\omega = 5$ , the temperature profile is almost superimposed on a temperature profile that is obtained by taking the upper time limit  $t = 10000$  s or  $\omega = 250$ . Evaluating a transverse line defined by  $\xi = 0$  mm and  $z = 10$  mm, Fig. 5 shows temperatures profiles which are already superimposed on each other even since temperature limit is 100 s or  $\omega = 2.5$ . These results enhance the previous conclusion that it is valid to take upper limit of non dimensional integration to 5.

$$T - T_0 = \dot{q} v / (4r_0^2 k \alpha \pi^{3/2}) \cdot \exp(-\xi V) \cdot \int_{r_0}^r r dr \cdot \int_{\omega=0}^{v^2 t / 4\alpha} I_0\left(r_0 V^2 / (2\omega) \sqrt{(\xi + 2\omega/V)^2 + y^2}\right) \exp\left(-\left(\omega + u^2/(4\omega)\right)\right) \frac{d\omega}{\omega^{3/2}} \quad (19)$$

$$T - T_0 = \dot{q} v / 8k\alpha\pi^{3/2} \cdot \exp(-\xi V) \cdot \int_{\omega=0}^{v^2 t / 4\alpha} I_0\left(r_0 V^2 / (2\omega) \sqrt{(\xi + 2\omega/V)^2 + y^2}\right) \exp\left(-\left(\omega + u^2/(4\omega)\right)\right) \frac{d\omega}{\omega^{3/2}} \quad (20)$$

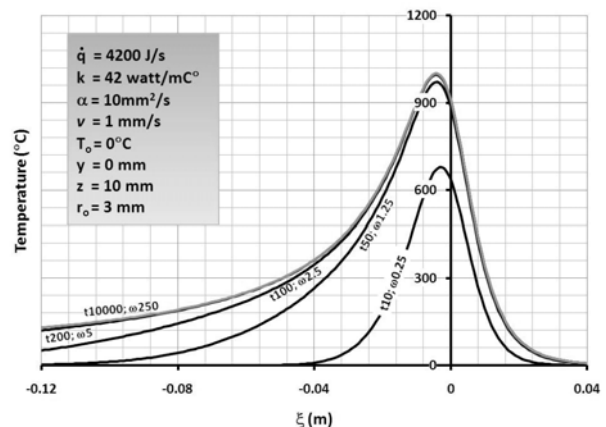


Fig. 4 Temperature profile at a longitudinal line

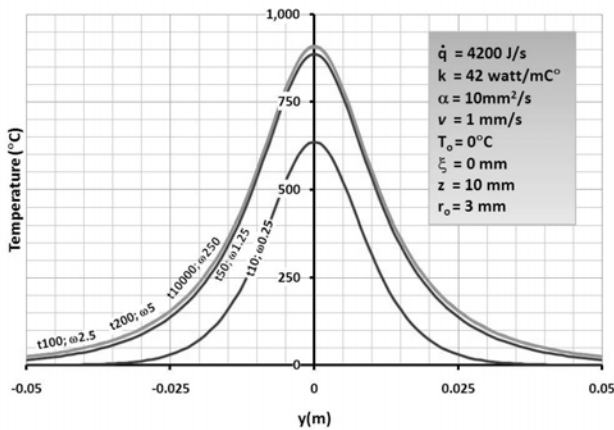


Fig. 5 Temperature profile at a transversal line

### III. FINITE ELEMENT METHOD

Basically, finite element method (FEM) considers a structure is constructed from simple elements which are connected at their nodes and fulfills equilibrium and compatibility conditions. Based on this definition, the first step at FEM is dividing an observed structure into elements.

Relation between temperatures and heats is obtained by applying virtual temperature principle in equilibrium equation which is expressed by (21).

$$\int_V \{\nabla T\}^T [k] \{\nabla T\} dV = \int_V T \dot{q}''' dV + \int_A T \dot{q}'' dA + \sum_i T \dot{q}' \quad (21)$$

Elements of conductance matrix [k] are obtained by evaluating compatibility equation at element model. The conductance matrix for a structure is obtained by assemble conductance matrix of its elements. Since a structure typically is comprised of huge number of elements, computer involvement is needed.

Finite element analysis was carried out using ANSYS 12.0 software. There are two options which can be used: ANSYS Parametric Design Language (APDL) and Graphic User Interface (GUI). In this paper APDL mode was chosen since flexibility and greater ease of modification is provided.

Again there are three types of heat source to describe welding torch; point heat source [9]-[11], surface heat source [12]-[14] and volumetric heat source [1],[15]. In this paper the heat source model used were again the point heat source and the uniformly distributed disc heat source.

First, FEM analysis uses moving point heat source model. The model is comprised of 23328 SOLID70 thermal elements with 26011 nodes to describe 250mm x 180mm x 90mm block. The heat source move along line (x,0,0) with x value changes according to time (Fig. 6). Typical welding parameters were chosen as follow: heat rate  $\dot{q} = 4200 J / s$ ,

thermal conductivity  $k = 42 \text{ watt/(m.C}^\circ)$ , thermal diffusivity  $\alpha = 10 \text{ mm}^2/\text{s}$  and welding speed  $v = 1 \text{ mm/s}$ .

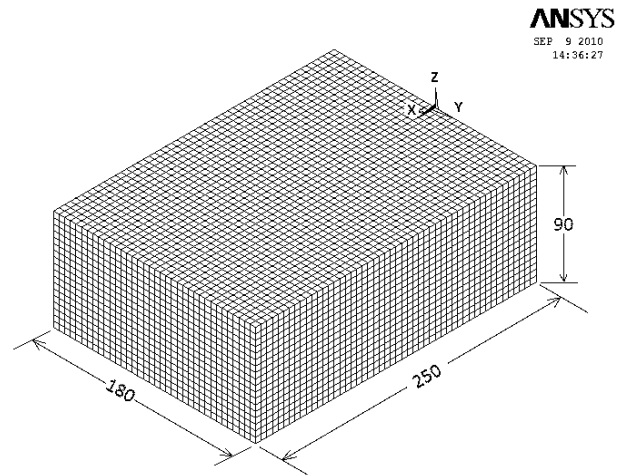


Fig. 6 FEM model for point heat source

The moving point heat source is modeled by a heat source at certain point and heat is liberated for certain time duration depend on welding speed and distance between two consecutive nodes. The distance is determined by mesh size of FEM model. After chosen duration the heat source is omitted and relocated to the next position where it liberates heat for the chosen duration. This procedure is repeated until the end of the weld length. Temperature profiles are observed after the heat source travels 200mm length (200s). Since  $\omega$  in this position is equal to 5, the temperature profiles can be considered as quasi steady condition for comparison with the analytic solution.

For the surface disc heat sources model, a simple geometric model as shown in Fig. 6 cannot be used. The mesh configuration for the disc heat source model is shown at Fig. 7 and magnified detail view is presented at Fig. 8. Finer meshes are needed in the area which is closer to the weld center line so that the surface disc heat source (circle area) can be closely represented by the meshes. Coarser meshes are used in area more remote from weld center line to save computer time.

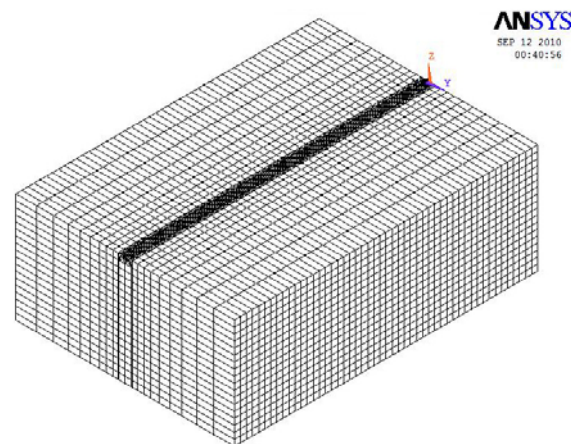


Fig. 7 FEM model for surface disc sources.

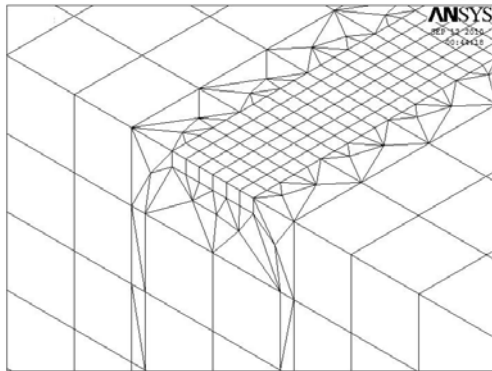


Fig. 8 Magnified detail view

The disc heat source in this model is described by a number of squares, one of the bricks element side. To describe a circular with radius 3mm around 36 squares are used. A total number of 37361 SOLID70 thermal elements with 27042 nodes were used and same parameters as used for the point heat source were applied.

#### IV. RESULTS AND DISCUSSIONS

For the point heat source the results are presented in Fig. 9 for longitudinal lines and at Fig.10 for transverse lines. Temperature profiles are evaluated at  $z = 0$  (at plate surface),  $z = 10$ ,  $z = 20$  and  $z = 30$  (under surface). On these lines temperatures were evaluated by both analytic solution and FEM, and the results are shown graphically in Fig. 9 and Fig. 10. Solid lines describe solutions provides by analytic solution and markers describe the solution provided by FEM. From Fig. 9 and Fig. 10 it can be seen that FEM provides results which are in good agreement with the analytic solutions, especially for points which are far enough away from point heat source.

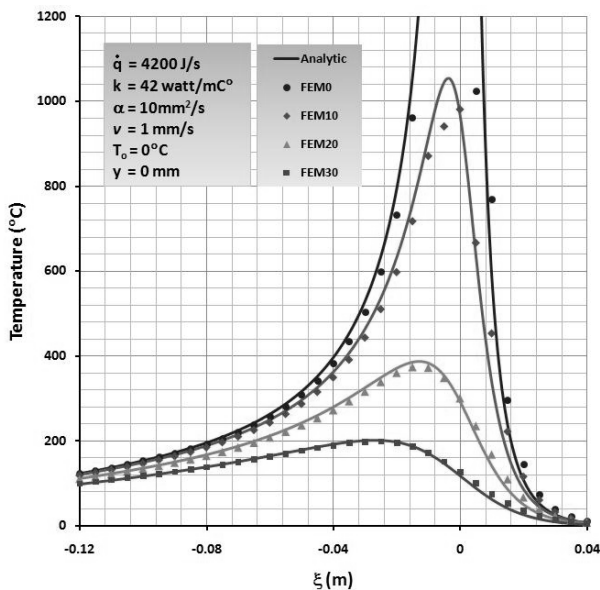


Fig. 9 Temperature profiles on longitudinal lines with moving point heat source model

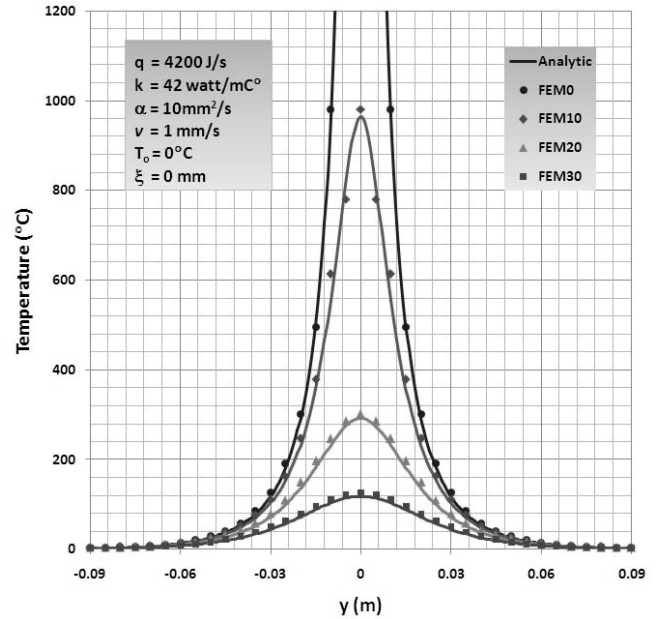


Fig. 10 Temperature profiles on transversal lines with moving point heat source model

Fig. 9 represents temperature profiles at  $y = 0$  with varied  $z$  values (see Fig. 1 for the axis nomenclature). The analytic solutions and FEM are in better agreement for temperature data behind the heat source model. Both analytic solutions and FEM can describe peak temperature which lags for higher values of  $z$  (the peak temperature is at negative  $\xi$  values); as it found in practice, since a longer time is needed to transfer heat from the heat source to higher  $z$  values (due to the longer distance). Meanwhile for certain minus value of  $\xi$  heat that is liberated from previous positions has reached the point on the observed line with the same minus  $\xi$  value. Transverse line shown in Fig. 10 are lines with  $\xi = 0$  with varied  $z$  values. Symmetric graphs are shown in Fig. 10. This symmetry is provided because  $\xi$  has the same value. It can be concluded from equation (12) that unsymmetrical function is provided by  $e^{-\xi V}$  term and only has effect when  $\xi$  is varied because the value of  $V$  ( $V=v/(2\alpha)$ ) depends on the welding parameters: welding speed ( $v$ ) and thermal property of material (diffusivity,  $\alpha$ ) which are considered constant.

Temperature values at  $y = 0$  in Fig. 10 should have the same values as those at  $\xi = 0$  in Fig. 9 since it shows the same points. It should however be underlined that peak temperatures in Fig. 10 are not the same as the peak temperatures in Fig. 9 as results of lagging effect discussed above.

The results for a uniformly distributed disc heat source model are shown at Fig.11 and Fig.12. The differences between analytic solutions and FEM results are higher than those for the point heat source. This may as a result of the use of non uniform meshes in the FEM model of the disc heat source (Fig. 7, Fig. 8) which cannot be avoided. Comparing Fig.9 with Fig.11 and Fig.10 with Fig.12 illustrates the difference between results for the point heat source model and

uniformly distributed disc heat source model using both analytic and FEM methods are practically insignificant.

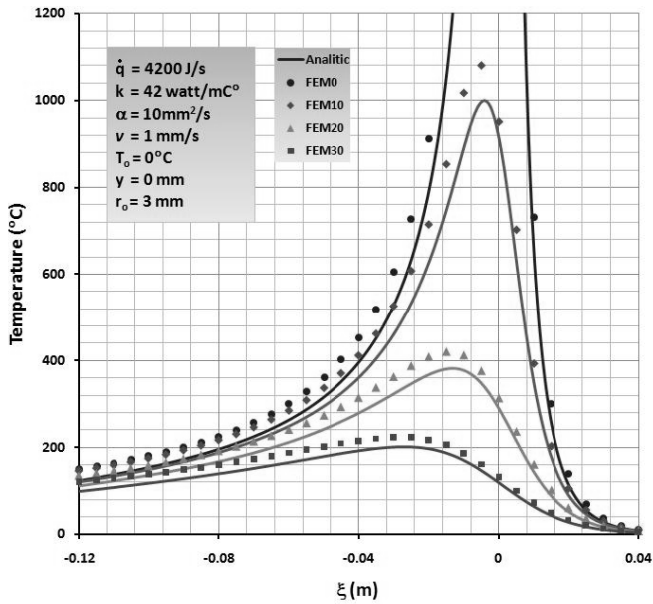


Fig. 11 Temperature profiles on longitudinal lines with uniformly distributed disc heat source model

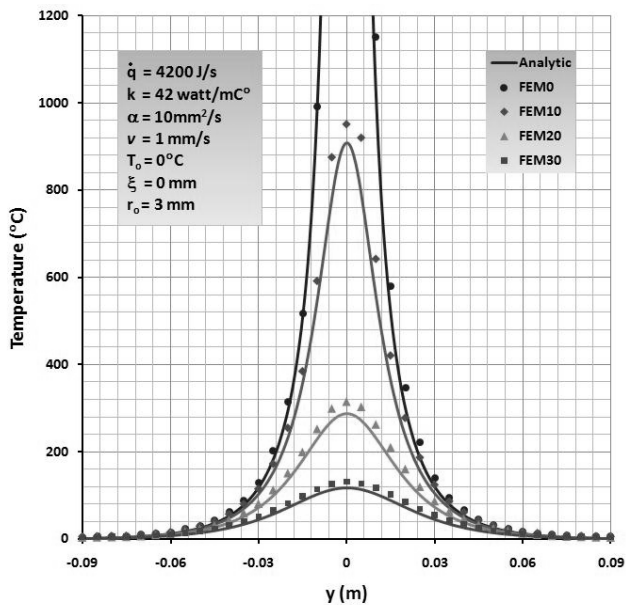


Fig. 12 Temperature profiles on transversal lines with uniformly distributed disc heat source model

Temperature profiles obtained from developed solutions which are expressed in (11) for point heat source model and in (18) for uniform disc heat source model are compared with Rosenthal solution (2). The comparison is presented graphically as in Fig.13 for transversal paths and Fig. 14 for longitudinal paths. From Fig.13 it can be said that for far field solutions no significant difference between developed solutions and Rosenthal whilst from Fig.14 for far field solutions behind the heat source there is a difference between

Rosenthal solution and developed solutions. In Fig.15 comparison is made between the analytic point heat source, Rosenthal and FEM for the far field solutions behind heat source. In Fig.14 only proposed solution based on point heat source is presented. At least there are two reasons for the absence of solution based on uniform disc heat source model: first from Fig.14 it can be seen that there is no significant difference for far field solutions between point heat source and uniform disc heat source, and the second reason is that Rosenthal based his solution on point heat source model. Fig.15 shows that the developed solution is confirmed by FEM whilst Rosenthal solution shows few higher temperatures.

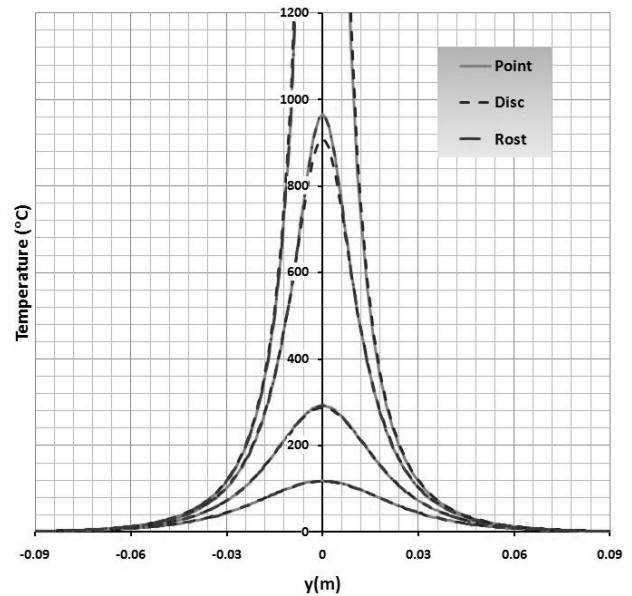


Fig. 13 Temperature profiles at transversal lines obtained from Rosenthal and developed solution based on point heat source model and uniform heat source model

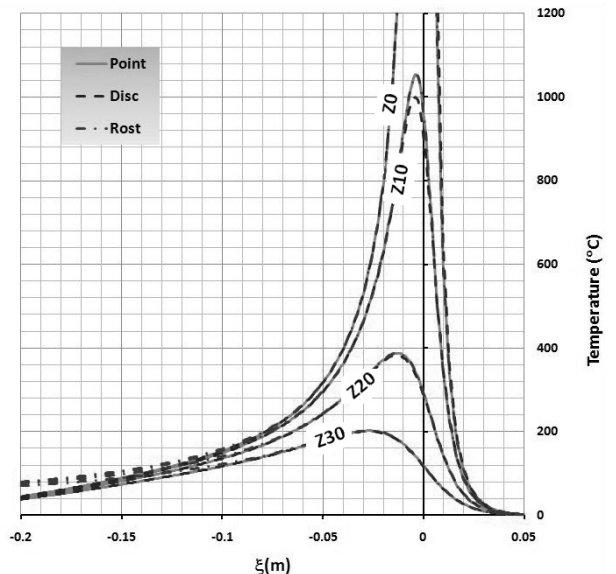


Fig. 14 Temperature profiles at longitudinal paths obtained from Rosenthal and developed solution based on point heat source model and uniform heat source model



The temperature profile difference as a result of different heat source model may however be seen in the area very closed to the heat source. The analytic result for the area adjacent to the heat source is presented in Fig. 16 and Fig. 17. Fig. 16 represents longitudinal observed lines with  $y = 0\text{mm}$  and  $z = 0\text{mm}$  (a closest longitudinal path) whilst Fig. 17 for transversal path with  $\xi = 0\text{mm}$  and  $z = 0\text{mm}$  (a closest transversal path). In Fig. 16 the temperature at  $\xi = 0$  has same value as the temperature at  $y = 0$  in fig. 17 for the specific heat source model applied. The solutions by FEM are not presented here since very fine meshes are needed and a large model should be provided to exhibit quasi steady state condition. Evaluating those figures it can be concluded that moving point heat source model gives higher temperature elevation than uniformly distributed moving disc heat source at positions very closed to the weld center. Results from both results are lower than temperature results obtained from Rosenthal solution which heading toward infinity.

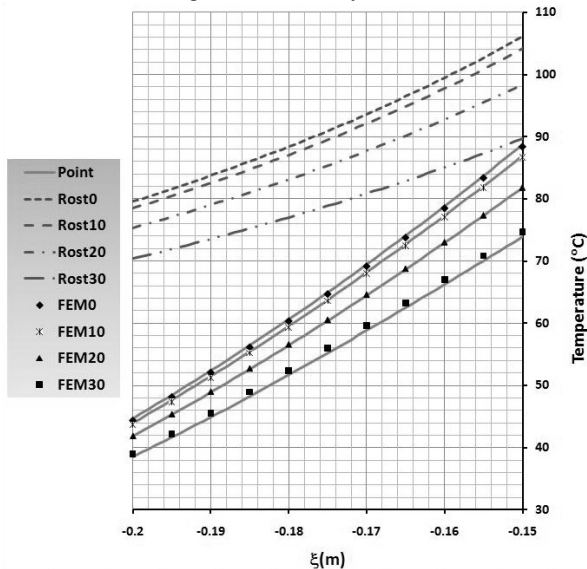


Fig. 15 Temperature profiles obtained from Rosenthal, analytic point heat source model and FEM solution

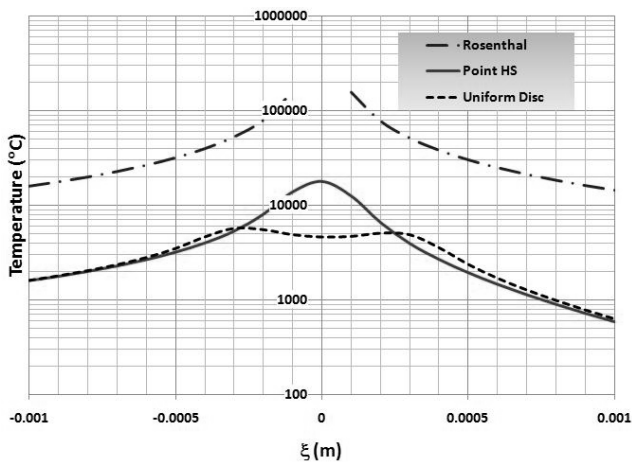


Fig. 16 Temperature profile on a longitudinal line with very close observed points to weld center

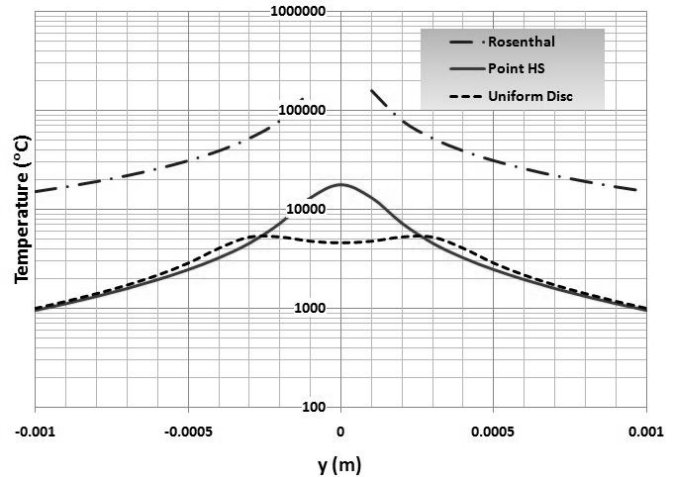


Fig. 17 Temperature profile on a transversal line with very close observed points to weld center

## V. CONCLUSIONS

The temperature profiles observed on longitudinal and transversal lines using both analytic and FEM method are in a good agreement. No significant temperature difference is found for positions remote from weld center using both point heat source and uniformly distributed disc heat source.

Comparing to the solution proposed by Rosenthal for point heat source model, the proposed analytic solution is closer to temperature profiles provided by FEM method. It is found especially at remote position behind the heat source center.

## VI. NOMENCLATURE

- $\alpha$  diffusivity ( $\text{m}^2/\text{s}$ )
- $\phi$  a function depend on heat load and material thermal properties
- $\rho$  density ( $\text{kg}/\text{m}^3$ )
- $\xi$  moving coordinate abscissa parallel to x axis
- $\nabla$  partial differential operator  $\left( \frac{\partial}{\partial x} \quad \frac{\partial}{\partial y} \quad \frac{\partial}{\partial z} \right)^T$
- $c$  specific heat ( $\text{J}/\text{kg}\cdot\text{C}^\circ$ )
- $I_0(p)$  modified Bessel function first kind, order zero
- $k$  thermal conductivity ( $\text{watt}/\text{m}\cdot\text{C}^\circ$ )
- $\dot{q}$  heat rate ( $\text{J}/\text{s}$ )
- $\dot{q}''$  heat flux rate ( $\text{J}/\text{sm}^2$ )
- $\dot{q}'''$  heat rate generated at a body ( $\text{J}/\text{sm}^3$ )
- $r, r_o$  ring radius, outer disc radius (m)
- $t, \tau$  time, time increment (s)
- $T, T_o$  temperature, initial temperature ( $^\circ\text{C}$ )
- $v$  welding speed (m/s)

## REFERENCES

- [1] Lei Yu-cheng, Yu Wen-xia, Li Chai-hui and Cheng Xiao-nong, "Simulation on temperature field of TIG Welding of cooper without preheating", Transaction of Nonferrous Metals Society of China, Vol.16, pp. 838-843, 2006.



- [2] Viorel Deaconu, Finite Element Modeling of Residual Stress – A Powerful Tool in The Aid of Structural Integrity Assessment of Welded Structures, 5th Int. Conference Structural Integrity of Welded Structures, Romania; 2007.
- [3] D. Rosenthal, “The theory of moving source of heat and its application to metal transfer”, Trans. ASME, vol.43 no.11, 1946.
- [4] H.S. Carslaw and J.C. Jaeger, “Conduction of heat in solid”, Clarendon Press, Oxford, 1959.
- [5] Z. Paley, J.N. Lync and Adam C.M. Jr, “Heat flow in welding heavy steel plate”, Welding Research Supplement, pp.71-79, 1964.
- [6] N. Christensen, V. Davies and K. Gjermundsen, “Distribution of temperature in arc welding”, British Welding Journal 12(2), pp. 54-75, 1965.
- [7] C.L. Tsai, “Heat flow in fusion welding”, Proceeding of the conference on trends in welding research in the united states, ASM International, New Orleans, pp.91 – 108, 1982.
- [8] R. Komanduri and Z.B. Hou, “Thermal analysis of the arc welding process: part I. General solutions”, Metallurgical and Materials Transactions, vol. 31B, pp. 1353 – 1370, 2000.
- [9] S. Dragi and V. Ivana, “Finite element analysis of residual stress in butt welding two similar plates”, Scientific Technical Review, vol.59, no.1, pp. 57-60, 2009.
- [10] M. Van Elsen, M. Baelmans, P. Mercelis and J.P. Kruth, “Solutions for modeling moving heat sources in a semi-infinite medium and application to laser material processing”, International Journal of Heat and Mass Transfer, vol.50, pp.4872 – 4882, 2007.
- [11] S. Dragi and V. Ivana, “Finite element analysis of residual stress in butt welding two similar plates”, Scientific Technical Review, vol.59, no.1, pp. 57-60, 2009.
- [12] Z. Chai, H. Zhao and A. Lu, “Efficient finite element approach for modeling of actual welded structures”, Science and Technology of Welding and Joining, vol.8, no.3, pp. 195 – 204, 2003.
- [13] F. Lu, S. You, S. Lou and Y. Li, “Modeling and finite element analysis on GTAW arc and weld pool”, Computational Materials Science, vol.29, pp. 371-378, 2004.
- [14] D. Dean & M. Hidekazu, “Prediction of welding residual stress in multi-pass butt-welded modified 9Cr-1Mo steel pipe considering phase transformation”, Computational Materials Science, vol.47, pp. 209-219, 2006.
- [15] X. Shan, C.M. Davies, T. Wangsdan, N.P. O’Dowd and K.M. Nikbin, “Thermo-mechanical modeling of a single-bead-on-plate weld using the finite element method”, International Journal of Pressure Vessels and Piping, vol. 86, pp. 110 – 121, 2009.